

# ICT: Image-Object Cross-Level Trusted Intervention for Mitigating Object Hallucination in Large Vision-Language Models

Junzhe Chen<sup>1,2\*</sup>, Tianshu Zhang<sup>1\*</sup>, Shiyu Huang<sup>3</sup>, Yuwei Niu<sup>4</sup>,  
Linfeng Zhang<sup>5</sup>, Lijie Wen<sup>1†</sup>, Xuming Hu<sup>2†</sup>

<sup>1</sup>Tsinghua University, <sup>2</sup>The Hong Kong University of Science and Technology (Guangzhou),  
<sup>3</sup>Zhipu AI, <sup>4</sup>Chongqing University, <sup>5</sup>Shanghai Jiao Tong University.

chenjz24@mails.tsinghua.edu.cn,  
wenlj@tsinghua.edu.cn, xuminghu97@gmail.com,

## Abstract

Despite the recent breakthroughs achieved by Large Vision Language Models (LVLMs) in understanding and responding to complex visual-textual contexts, their inherent hallucination tendencies limit their practical application in real-world scenarios that demand high levels of precision. Existing methods typically either fine-tune the LVLMs using additional data, which incurs extra costs in manual annotation and computational resources or perform comparisons at the decoding stage, which may eliminate useful language priors for reasoning while introducing inference time overhead. Therefore, we propose ICT, a lightweight, training-free method that calculates an intervention direction to shift the model’s focus towards different levels of visual information, enhancing its attention to high-level and fine-grained visual details. During the forward pass stage, the intervention is applied to the attention heads that encode the overall image information and the fine-grained object details, effectively mitigating the phenomenon of overly language priors, and thereby alleviating hallucinations. Extensive experiments demonstrate that ICT achieves strong performance with a small amount of data and generalizes well across different datasets and models. Our code will be public.

## 1. Introduction

The recent rapid advancements in Large Vision Language Models (LVLMs) have demonstrated significant potential to tackle complex real-world tasks [5, 27, 29, 52, 56]. However, LVLMs frequently generate text outputs that are inconsistent with the visual input, such as incorrectly determining the presence of objects in an image or inaccurately describing the attributes of those objects [55, 72]. This

\* Equal Contribution.

† Corresponding authors.

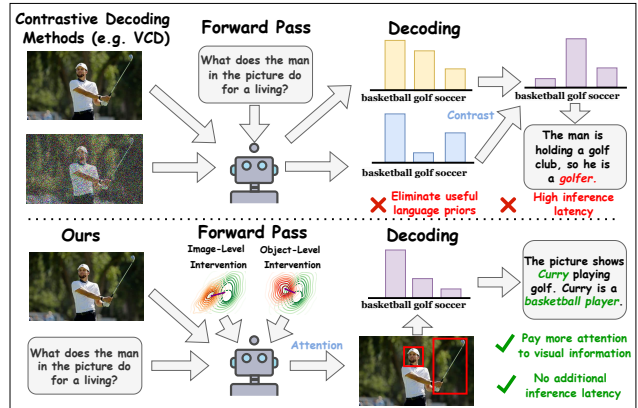


Figure 1. Comparison between Contrastive Decoding (top) and our proposed ICT (bottom). In the top example, Contrastive Decoding indiscriminately removes both beneficial and detrimental language priors, leading to hallucinations. In contrast, our approach enhances the model’s attention to visual details while preserving useful language priors, allowing it to correctly identify and describe objects in the image.

issue is commonly referred to as the *object hallucination phenomenon* [55], which significantly limits the applicability of LVLMs in high-stakes scenarios that demand precise accuracy, such as autonomous driving [94] and medical surgery [35, 82]. Previous research suggested that the primary reasons for hallucinations in LVLMs are as follows: 1) Large language models (LLMs), such as Vicuna [12], possess significantly stronger parameters and capabilities compared to visual encoders, such as CLIP [67]. This results in an excessively strong language prior, causing the model to overly rely on language cues while neglecting visual input [24, 25, 40, 43, 55]. 2) Current visual decoders often struggle to accurately capture fine-grained visual semantics, resulting in errors in detailed object attributes in an image, such as color and quantity [4, 9, 13, 55].

Based on the two issues outlined above, previous efforts to mitigate the hallucination phenomenon in LVLMs

can be categorized into three main approaches: 1) **Fine-tuning with additional data:** This approach involves introducing high-quality annotated data to better align the model’s behavior with human interpretations, effectively teaching the model to focus more on visual information [23, 46, 52, 104]. However, this method not only requires costly human annotation but also involves updating model parameters, which demands substantial computational resources, thereby limiting its scalability. 2) **Perceptual enhancement:** This method incorporates additional information, such as depth maps and segmentation maps [34, 38, 104], as auxiliary inputs to assist the visual encoder in capturing more detailed visual features, thereby reducing hallucinations. However, it often requires manual selection of auxiliary features, which limits its generalizability across different tasks. 3) **Contrastive decoding:** This method alleviates hallucinations without requiring additional training. It induces hallucinations by applying transformations such as blurring, rotation, or cropping to the original visual input. During the decoding stage, tokens associated with these induced hallucinations are penalized, thus mitigating the influence of language priors [10, 14, 36, 43, 63, 69, 81, 86, 107]. However, methods such as VCD often indiscriminately eliminate all language priors, including those that may be beneficial. As shown in Figure 1, the original model recognizes Curry holding a golf club, while utilizing the language prior that identifies Curry as a basketball player. This language prior is valuable for achieving an accurate interpretation. However, through contrastive decoding, this useful prior is also removed, which can inadvertently result in hallucinations.

To address the challenges of mitigating hallucinations in LVLMs, we propose **Image-Object Cross-Level Trusted Intervention (ICT)**, a training-free, plug-and-play method applicable during the forward pass. Unlike contrastive decoding, our approach does not eliminate language priors to reduce the model’s over-reliance on text modality. Instead, it intervenes during the forward pass to enhance the model’s focus on both comprehensive visual information and fine-grained object details. We explored the activation patterns of attention heads when the model produces correct versus hallucinated responses. This analysis allowed us to identify activation value deviations that can shift the model from being “untrustworthy” to “trustworthy”. According to prior research [8, 19, 80], which has shown that different heads in the multi-head attention mechanism encode information at varying levels of granularity, we train binary classifiers for each head to determine which heads encode overall visual information and which capture detailed visual features. During the forward pass, we adjust the activation values of these heads based on their identified levels, thereby enhancing the model’s attention to the relevant visual features and reducing the likelihood of hallucinations. As illustrated in

Figure 1, after applying ICT, the model is able to focus more on the details within the image, such as identifying the man as Curry, while simultaneously utilizing beneficial language priors (e.g., Curry is a basketball player) to infer and arrive at the correct answer. Since the intervention shift vectors are pre-computed, ICT does not introduce additional delays during the forward pass.

Our experiments demonstrate that, for both LLaVA-v1.5 [52] and Qwen-VL [5], applying ICT results in an average improvement of 6.27% on POPE benchmark and 67.37 points on MME benchmark. Furthermore, ICT exhibits cross-dataset generalization and model-agnostic generalizability. Our contributions can be summarized as:

- We propose **Image-Object Cross-Level Trusted Intervention (ICT)**, a novel, training-free, plug-and-play method that effectively reduces hallucinations in LVLMs by enhancing focus on both overall visual information and fine-grained object details during the forward pass, without eliminating beneficial language priors.
- Unlike existing contrastive decoding approaches, we introduce an intervention mechanism that operates during the forward pass rather than the decoding stage, allowing ICT to be orthogonal and complementary to existing decoding strategies while not introducing any additional latency.
- Extensive experiments on LLaVA-v1.5 and Qwen-VL demonstrate that ICT significantly improves performance on both the POPE and MME benchmarks while maintaining cross-dataset and model-agnostic generalizability.

## 2. Related Work

### 2.1. Large Vision-Language Models

Following the success of LLM [6, 12, 60, 77, 79], researchers have been exploring the multimodal field. Taking advantage of the remarkable capabilities of LLMs, Large Vision-Language Models incorporate visual encoders and feature projectors into powerful LLMs, enabling them to understand and generate content based on visual and text input. Most of these models undergo two training steps, namely the pre-training stage and the fine-tuning stage. The main purpose of the pre-training stage is to align textual and visual features, while the goal of the fine-tuning stage is to bridge further the modality gap between vision and language, as well as lifting their instruction following capabilities and performance on specific downstream tasks. Early attempts, such as FLamingo [2], Gemini [78], and BLIP-2 [44], have already shown promising results. Recent works like LLaVA-v1.5 [54], Qwen2-VL [83], and xgen-mm [91] have advanced this field, dramatically improving the abilities of these models. To enhance the consistency between vision representation and language representation, many efforts have been made, including utilizing higher resolution vision encoders, transitioning to larger and more

capable LLMs, and adapting reinforcement learning techniques such as RLHF [61, 97], among others. Despite the remarkable progress that has been made, LVLMs still suffer from severe hallucinations, which restricts their potential for large-scale applications in real-world scenarios.

## 2.2. Mitigating Hallucinations in LVLMs

Many efforts have been made to understand the causes of hallucination [1, 16, 30, 39, 50, 50, 53, 62, 64, 70, 71, 75, 92, 99]. Existing approaches to mitigate hallucinations can be roughly divided into two categories based on the stage they take place. The first category focuses on the training phase. Most of the work falling into this category introduces additional or curated datasets [21, 22, 51, 96], these works usually design a dataset specifically for hallucination-related tasks or improve data cleaning methods [68, 74], or introduce novel training objectives [7, 41, 76]. While effective, these methods typically require extensive training, which is both time-consuming and resource-intensive. The second category focuses on the inferencing phase, usually involves CD-based [47] novel decoding strategies [10, 14, 36, 58, 63, 69, 81, 86, 93, 105, 107]. Another approach is to detect potential hallucinations while generating and correct them [18, 37, 59], among others [45, 85, 98, 101]. In addition, some researchers tackle hallucinations by manipulating attention weight assigned to the image [33, 88, 89, 102, 106], or the prompt-related part of the image [3]. Other works include prompt-based methods [42, 66, 84, 87, 90, 100], utilizing external tools [11, 95, 103] or external knowledge [17, 28, 65] and so on.

However, one of the most vital features for large vision-language models, *i.e.* the activation space in the inferencing stage, remains severely underexploited. Consequently, our study seeks to conduct head-level intervention during the inferencing stage, paving the way for more effective applications of large vision-language models.

## 3. Task Formulation

Given an LVLM parameterized by  $\theta$ , the model processes a textual input  $\mathbf{X} = \{x_1, x_2, \dots, x_{N_x}\}$  and a visual input  $\mathbf{V} = \{v_1, v_2, \dots, v_{N_v}\}$ , where  $N_x$  and  $N_v$  denote the sequence lengths of the text and visual inputs, respectively. The model then concatenates the textual and visual sequences to form a unified input  $\mathbf{H} = \text{concat}(\mathbf{Y}, \mathbf{X})$ , which is subsequently passed through  $L$  layers of a transformer architecture. At each layer, the concatenated input undergoes multi-head attention, which is computed as:

$$\mathbf{H}^{(l+1)} = \mathbf{H}^{(l)} + \sum_{n=1}^N \text{Attn}_n^{(l)}(\mathbf{H}^{(l)}) \cdot \mathbf{W}_o^{(l)}, \quad (1)$$

where  $\text{Attn}_n^{(l)}$  denotes the attention operation of the  $n$ -th head at the  $l$ -th layer, and  $\mathbf{W}_o^{(l)} \in \mathbb{R}^{d \times Nd}$  is the output

projection matrix, with  $d$  representing the dimensionality of each attention head and  $N$  the number of heads. Subsequently, the model autoregressively predicts the next token based on the output from the  $L$ -th layer:

$$p(y_t | y_{<t}) = \text{Softmax}(fc(\mathbf{H}_t^{(L)})), \quad (2)$$

where  $fc(\cdot)$  is an affine layer mapping the  $Hd$ -dimensional vector to a probability distribution of vocabulary size  $M$ .

## 4. Methodology

In this section, we introduce two levels of fine-grained intervention modules. The first module enables the LVLM to focus on the image, thereby reducing over-reliance on language priors. The second module encourages the LVLM to attend more closely to image objects, helping to mitigate the omission of critical objects and reduce hallucinations.

### 4.1. Intervention at Image-Level

This module aims to identify the attention heads associated with overall image information and to apply targeted interventions to these heads. This approach enhances the model’s focus on visual input while diminishing the influence of language priors.

As illustrated in Figure 2, consider a batch of image-question pairs, denoted as  $\{(X_i, V_i)\}_{i=1}^B$ , each labeled with the answer “Yes” from the POPE dataset. Here,  $X_i$  takes the form of “Is there a/an [object] in the image?” For each question, we extract the specified object  $O_i$  and reformulate the question to  $q =$  “What is it in the image?” Then, for each image  $V_i$ , we progressively add Gaussian noise following the forward diffusion process [26] to obtain the final blurred image  $V_i'$ :

$$q(V_i^{(t)} | V_i^{(t-1)}) = \mathcal{N}(V_i^{(t)}; \sqrt{1 - \beta_t} V_i^{(t-1)}, \beta_t \mathbf{I}),$$

$$q(V_i' | V_i) = \prod_{t=1}^T q(V_i^{(t)} | V_i^{(t-1)}), \quad (3)$$

where  $\beta_t$  is the noise variance at step  $t$ . Finally, we construct a modified dataset  $\{(q, V_i, V_i', O_i)\}_{i=1}^B$  to obtain Image-Level intervention vectors. We then concatenate  $O_i$  with the question  $q$  to form the answer, resulting in data pairs of trusted and untrusted data for the same sample:  $(q + O_i, V_i)$  and  $(q + O_i, V_i')$ . For each sample, we treat the representation of the last token as the fused representation of multimodal data and extract the attention activation from a total of  $N \times L$  heads across the  $L$  layers for both trusted and untrusted data. These are denoted as  $A_i = \{\text{Attn}_n^{(l)} \mathbf{H}_s^{(l)}\}_{n=1, l=1}^{N, L}$  and  $A_i' = \{\text{Attn}_n^{(l)} \mathbf{H}'_s^{(l)}\}_{n=1, l=1}^{N, L}$ , where  $s = N_x + N_v + 1$ . According to the trusted activation  $\{A_i\}_{i=1}^B$  and the untrusted activation  $\{A_i'\}_{i=1}^B$  obtained from all sample pairs, we can calculate the following activation shift vector  $\{\mathbf{S}_n^{(l)}\}_{n=1, l=1}^{N, L}$  that encourages the model

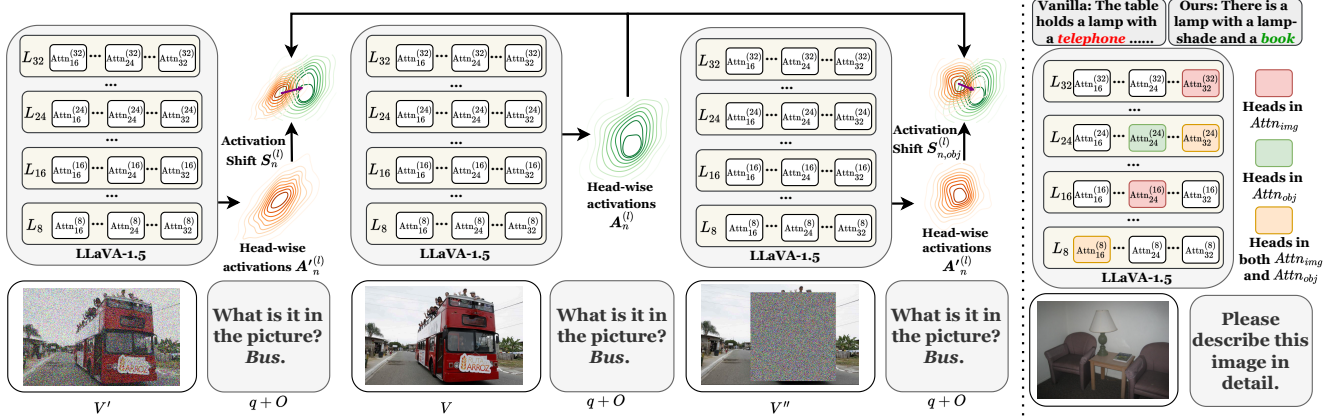


Figure 2. Overview of our proposed ICT method. ICT consists of two levels of intervention: Image-Level and Object-Level. The Image-Level module enhances the model’s focus on the overall scene to reduce reliance on language priors, while the Object-Level module focuses on fine-grained details to mitigate hallucinations. We apply targeted activation shifts to selected attention heads identified through binary classifiers trained to distinguish trusted and untrusted data pairs.

to pay more attention to visual information, as follows:

$$\mathbf{S}_n^{(l)} = \frac{1}{B} \sum_{i=1}^B \left( \mathbf{A}_{i,n}^{(l)} - \mathbf{A}'_{i,n} \right). \quad (4)$$

Next, we train a binary classifier  $f_n^{(l)}(\cdot)$  using  $B$  sample pairs for each head to detect which heads encode Image-Level information, specifically those that can better distinguish the differences between pairs of trusted and untrusted samples. We then apply activation interventions to these selected heads:

$$\begin{aligned} \text{Attn}_{\text{img}} &= \{ \text{Attn}_n^{(l)} \mid \text{Attn}_n^{(l)} \in \text{TopK}(\text{Accuracy}(f_n^{(l)}(\cdot))) \}, \\ \mathbf{H}^{(l+1)} &= \mathbf{H}^{(l)} + \sum_{n=1}^N \left( \text{Attn}_n^{(l)}(\mathbf{H}^{(l)}) + \mathbb{I}_{\text{img},n}^{(l)} \alpha \mathbf{S}_n^{(l)} \right) \cdot \mathbf{W}_o^{(l)}, \end{aligned} \quad (5)$$

where  $K$  is the number of selected intervention heads,  $\mathbb{I}_{\text{img},n}^{(l)}$  is an indicator function, which is 1 if  $\text{Attn}_n^{(l)} \in \text{Attn}_{\text{img}}$  and 0 otherwise, and  $\alpha$  denotes the intensity of the intervention. After using  $\{ \mathbf{S}_n^{(l)} \}_{n=1,l=1}^{N,L}$  to perform Image-Level interventions on heads that encode image information, the model enhances the trustworthiness of the visual level, places greater attention on visual information, thus mitigates the impact of overly strong language priors.

## 4.2. Intervention at Object-Level

After enhancing the model’s trustworthiness at the Image-Level, a more fine-grained, Object-Level intervention becomes necessary to increase the model’s attention to image details, thereby reducing hallucinations caused by the omission of fine details. As shown in Figure 2, similar to Section 4.1, we construct a dataset  $\{(q, V_i, V_i'', O_i)\}_{i=1}^B$  to obtain Object-Level intervention vectors. We use Grounding DINO [57] to identify the area of object  $O_i$  in image  $V_i$ .

Gaussian noise is then added selectively to this object region, based on Eq. 3, producing a locally blurred image  $V_i''$ . Using both the original image  $V_i$  and the partially blurred image  $V_i''$ , we construct trusted and untrusted data pairs for each sample:  $(q + O_i, V_i)$  and  $(q + O_i, V_i'')$  and analyze the attention activation values across  $N \times L$  heads, allowing us to compute an Object-Level activation shift vector  $\{ \mathbf{S}_{n,\text{obj}}^{(l)} \}_{n=1,l=1}^{N,L}$ :

$$\mathbf{S}_{n,\text{obj}}^{(l)} = \frac{1}{B} \sum_{i=1}^B \left( \mathbf{A}_{i,n}^{(l)} - \mathbf{A}''_{i,n} \right). \quad (6)$$

A binary classifier  $f_{n,\text{obj}}^{(l)}(\cdot)$  is then trained to identify heads that effectively distinguish trusted from untrusted object-focused samples. Interventions are subsequently applied to the selected heads as follows:

$$\begin{aligned} \text{Attn}_{\text{obj}} &= \{ \text{Attn}_n^{(l)} \mid \text{Attn}_n^{(l)} \in \text{TopK}(\text{Accuracy}(f_{n,\text{obj}}^{(l)}(\cdot))) \}, \\ \mathbf{H}^{(l+1)} &= \mathbf{H}^{(l)} + \sum_{n=1}^N \left( \text{Attn}_n^{(l)}(\mathbf{H}^{(l)}) + \mathbb{I}_{\text{obj},n}^{(l)} \beta \mathbf{S}_{n,\text{obj}}^{(l)} \right) \cdot \mathbf{W}_o^{(l)}, \end{aligned} \quad (7)$$

where  $K$  is the number of intervention heads,  $\mathbb{I}_{\text{obj},n}^{(l)}$  is an indicator function set to 1 if  $\text{Attn}_n^{(l)} \in \text{Attn}_{\text{obj}}$  and 0 otherwise, and  $\beta$  controls the intervention intensity.

Finally, we integrate the Image-Level and Object-Level intervention modules to create a unified approach that reinforces the model’s focus on both the overall visual context and finer object-specific details as follows:

$$\begin{aligned} \mathbf{H}^{(l+1)} &= \mathbf{H}^{(l)} + \sum_{n=1}^N \left( \text{Attn}_n^{(l)}(\mathbf{H}^{(l)}) \right. \\ &\quad \left. + \mathbb{I}_{\text{img},n}^{(l)} \alpha \mathbf{S}_n^{(l)} + \mathbb{I}_{\text{obj},n}^{(l)} \beta \mathbf{S}_{n,\text{obj}}^{(l)} \right) \cdot \mathbf{W}_o^{(l)}. \end{aligned} \quad (8)$$

By applying these interventions in tandem, the model gains a balanced attention mechanism that mitigates exces-

sive reliance on language priors while enhancing sensitivity to essential visual cues across different levels of granularity, thereby alleviating the occurrence of hallucinations.

## 5. Experiments

### 5.1. Experimental Setup

#### Datasets and Metrics.

**POPE** [48] (Polling-based Object Probing Evaluation) is a benchmark designed to assess how effectively LVLMS recognize the presence of specific objects in images, thus identifying Object-Level hallucinations. It uses Yes/No questions based on object annotations, with metrics including Accuracy, Precision, Recall, and F1 score. The dataset is balanced, with 50% of queries for existing objects and 50% for non-existing ones, and employs three sampling strategies: random, popular, and adversarial. Drawing from MSCOCO [49], A-OKVQA [73], and GQA [32] datasets, POPE evaluates 27,000 query-answer pairs to gauge model performance.

**MME** [20] (Multimodal Large Language Model Evaluation) benchmark is designed to comprehensively evaluate the performance of LVLMS across various dimensions. It includes ten perception-focused tasks and four cognition-related tasks. MME benchmark specifically addresses Object-Level hallucinations through subsets focusing on object existence and count, while attribute-level hallucinations are assessed via subsets related to object position and color. The evaluation metric is Accuracy, providing a quantitative measure of the model’s performance across these diverse tasks.

**Baselines.** We adopt the widely used LLaVA-v1.5 [52] and Qwen-VL [5] models as our baseline LVLMS. We compared two baselines that eliminate language priors of the LVLMS in the decoding stage to alleviate hallucinations: VCD [43] and Opera [31].

**Implementation Details.** In our experiments, we utilized 1,500 QA pairs with “Yes” responses from the COCO Random subset of the POPE dataset to train the intervention shift vector. Subsequently, we evaluated the ICT approach on two datasets with significant distributional differences: POPE, and MME. This evaluation was conducted to assess the generalizability and robustness of ICT across diverse data distributions. For each attention head, we employed Support Vector Machines (SVMs) [15] as the classifier and performed 2-fold cross-validation to evaluate the classification accuracy. In the experiment, we set  $\alpha = \beta$  and determined the optimal values of  $\alpha$ ,  $\beta$ , and  $K$  through a grid search. Detailed hyperparameter configurations are provided in Appendix A. All experiments were conducted on a system equipped with  $8 \times$  H800 GPUs.

### 5.2. Main Results

**Results on POPE.** Table 1 presents the results of LLaVA-v1.5 and Qwen-VL on nine subsets of the POPE dataset. From comparing these methods, we can derive the following conclusions: **1)** Applying ICT results in an average performance improvement on the F1 score for LLaVA-v1.5 and Qwen-VL of 7.09% and 5.44% on 9 subsets respectively, which are respectively higher than the previous contrastive decoding sota baseline (Opera) 2.19% and 1.14%. This improvement can be attributed to the fact that ICT does not eliminate language priors, which may provide useful information. Instead, it enhances the model’s attention to various levels of visual information, thereby reducing the model’s tendency to overly rely on language priors and mitigating the occurrence of hallucinations. **2)** Individually intervening at both the image level and object level, with average gains of 5.76% and 5.47% in F1 score, respectively. This demonstrates that enhancing LVLMS’ attention to image information at various levels can effectively mitigate hallucinations. Moreover, since Object-Level intervention also implicitly directs the model’s focus toward broader image information, it achieves a comparatively higher performance gain. **3)** The intervention shift vector trained using 1,500 samples from the MSCOCO random subset achieves an average improvement on F1 score of 7.67% on the MSCOCO random subset and an average improvement of 6.09% across the other eight subsets with different distributions. This indicates that ICT generalizes effectively, and the resulting intervention vector captures a general direction towards trustworthiness rather than merely fitting a specific dataset.

**Results on MME.** Figure 3 presents the experimental results on the MME benchmark, where we followed Leng et al. [43] evaluation setup, focusing on the hallucination subset of MME. Compared to the unmodified model, ICT achieved a score improvement of 80.51 on LLaVA-v1.5 and 34.67 on Qwen-VL, surpassing the performance of VCD. Additionally, on non-hallucination tasks such as common-sense QA, ICT demonstrated a 10-point improvement on LLaVA-v1.5 and a 9.5-point improvement on Qwen-VL. These results indicate that ICT not only effectively reduces hallucinations but also enhances general reasoning capabilities across different models. Moreover, since the objects present in the images of the MME dataset are generally prominent, the variant ICT *w/o* image (i.e., without the Image-Level intervention that enhances the model’s attention to the overall scene) provides only limited improvements compared to ICT *w/o* object. This demonstrates that the absence of Image-Level guidance restricts the model’s ability to fully leverage global visual context, thereby reducing its effectiveness in scenarios where the dominant objects play a crucial role.

Dataset	Setting	Method	LLaVA-v1.5		Qwen-VL	
			Accuracy	F1 Score	Accuracy	F1 Score
COCO	<i>Random</i>	Regular	83.29	81.33	84.37	82.67
		VCD	87.73	87.16	88.63	87.81
		OPERA	89.20	88.81	87.31	86.92
		ICT <i>w/o</i> image	<u>89.70 (+6.41)</u>	<u>89.93 (+8.60)</u>	88.76(+4.39)	87.84(+5.17)
		ICT <i>w/o</i> object	<u>88.50 (+5.21)</u>	<u>88.81 (+7.48)</u>	89.13(+4.76)	<u>88.20(+5.63)</u>
		ICT	<b>90.11 (+6.82)</b>	<b>90.03 (+8.70)</b>	<b>89.46(+5.09)</b>	<b>89.20(+6.63)</b>
	<i>Popular</i>	Regular	81.88	80.06	84.13	82.06
		VCD	85.38	85.06	87.12	86.40
		OPERA	86.64	86.62	87.44	86.68
		ICT <i>w/o</i> image	<u>87.43 (+5.55)</u>	<u>87.09 (+7.03)</u>	87.63(+3.50)	86.78(+4.72)
		ICT <i>w/o</i> object	<u>87.30 (+5.42)</u>	<u>86.65 (+6.59)</u>	87.10(+2.97)	86.28(+4.22)
		ICT	<b>87.50 (+5.62)</b>	<b>87.60 (+7.54)</b>	<b>88.16(+4.03)</b>	<b>87.33(+5.27)</b>
	<i>Adversarial</i>	Regular	78.96	77.57	82.26	80.37
		VCD	80.88	81.33	84.26	83.90
		OPERA	81.24	81.38	84.78	83.45
		ICT <i>w/o</i> image	<u>84.13 (+5.17)</u>	<u>83.31 (+5.74)</u>	85.13(+2.87)	84.35(+3.98)
		ICT <i>w/o</i> object	<u>83.63 (+4.67)</u>	<u>82.13 (+4.56)</u>	<b>85.23(+2.97)</b>	<b>84.62(+4.25)</b>
		ICT	<b>84.43 (+5.47)</b>	<b>83.74 (+6.17)</b>	84.96(+2.70)	84.42(+4.05)
AOKVQA	<i>Random</i>	Regular	83.45	82.56	86.67	85.59
		VCD	86.15	86.34	89.22	89.01
		OPERA	88.02	84.59	88.19	88.43
		ICT <i>w/o</i> image	<b>89.60 (+6.15)</b>	<b>89.75 (+7.19)</b>	<b>89.46(+2.79)</b>	<b>89.28(+3.69)</b>
		ICT <i>w/o</i> object	<u>89.00 (+5.55)</u>	<u>88.91 (+6.35)</u>	89.26(+2.59)	88.95(+3.36)
		ICT	<u>89.20 (+5.75)</u>	<u>89.41 (+6.85)</u>	<b>89.46(+2.79)</b>	<u>89.03(+3.44)</u>
	<i>Popular</i>	Regular	79.90	79.59	85.56	84.63
		VCD	81.85	82.82	87.85	<u>87.81</u>
		OPERA	83.22	84.67	87.91	87.13
		ICT <i>w/o</i> image	<u>85.36 (+5.46)</u>	<b>85.34 (+5.75)</b>	87.70(+2.14)	87.68(+3.05)
		ICT <i>w/o</i> object	<u>84.65 (+4.75)</u>	<u>84.32 (+4.73)</u>	87.90(+2.34)	87.48(+2.85)
		ICT	<b>85.73 (+5.83)</b>	<b>85.34 (+5.75)</b>	<b>88.13(+3.57)</b>	<b>87.83(+3.20)</b>
	<i>Adversarial</i>	Regular	74.04	75.15	79.57	79.50
		VCD	74.97	77.73	81.27	82.38
		OPERA	73.82	77.91	80.82	81.54
		ICT <i>w/o</i> image	<u>79.26 (+5.22)</u>	<u>80.14 (+4.99)</u>	81.50(+1.93)	82.10(+2.60)
		ICT <i>w/o</i> object	<u>77.79 (+3.75)</u>	<u>79.53 (+4.38)</u>	81.40(+1.83)	82.18(+2.68)
		ICT	<b>79.60 (+5.56)</b>	<b>80.43 (+5.28)</b>	<b>81.94(+2.37)</b>	<b>82.44(+2.94)</b>
GQA	<i>Random</i>	Regular	83.73	82.95	80.97	79.01
		VCD	86.65	86.99	85.59	85.33
		OPERA	88.13	88.91	86.02	85.29
		ICT <i>w/o</i> image	<u>89.03 (+5.30)</u>	<u>88.99 (+6.04)</u>	85.20(+4.23)	85.90(+6.89)
		ICT <i>w/o</i> object	<u>88.97 (+5.24)</u>	<u>89.30 (+6.35)</u>	<b>87.20(+6.23)</b>	86.80(+7.79)
		ICT	<b>89.60 (+5.87)</b>	<b>89.44 (+6.49)</b>	<u>86.38(+5.41)</u>	<b>86.96(+7.95)</b>
	<i>Popular</i>	Regular	78.17	78.37	75.99	74.84
		VCD	80.73	82.24	81.83	<u>82.23</u>
		OPERA	79.27	82.11	81.97	82.12
		ICT <i>w/o</i> image	<u>84.23 (+6.06)</u>	<u>83.92 (+5.55)</u>	81.43(+5.44)	80.86(+6.02)
		ICT <i>w/o</i> object	<b>84.70 (+6.53)</b>	<u>84.45 (+6.08)</u>	<b>83.93(+7.94)</b>	<b>82.95(+8.11)</b>
		ICT	<b>84.70 (+6.53)</b>	<b>84.78 (+6.41)</b>	<u>82.63(+6.64)</u>	82.22(+7.38)
	<i>Adversarial</i>	Regular	75.08	76.06	75.46	74.33
		VCD	76.09	78.78	80.01	<u>80.75</u>
		OPERA	75.00	78.71	80.24	80.64
		ICT <i>w/o</i> image	<b>81.92 (+6.84)</b>	<u>82.11 (+6.05)</u>	80.03(+4.57)	79.90(+5.47)
		ICT <i>w/o</i> object	<u>81.65 (+6.57)</u>	<u>82.00 (+5.94)</u>	<b>81.60(+6.14)</b>	<b>81.53(+7.10)</b>
		ICT	<u>81.50 (+6.42)</u>	<b>82.27 (+6.21)</b>	<u>80.83(+5.37)</u>	80.60(+6.17)

Table 1. **Main results on POPE tasks.** We evaluate the accuracy of various LVLMs on the POPE task across the MSCOCO, A-OKVQA, and GQA datasets. **Regular** represents the setting where direct sampling is applied. **ICT *w/o* image** and **ICT *w/o* object** correspond to the exclusion of image-level and object-level interventions, respectively. The **bold** and underlined values indicate the highest and second-highest metrics under each setting, respectively.

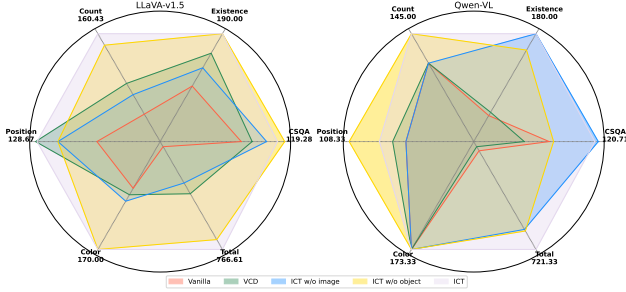


Figure 3. Comparison of ICT with baseline methods (Vanilla and VCD) on the MME benchmark. The radar chart illustrates improvements across various evaluation categories, including existence, position, color, and commonsense QA (CSQA).

## 6. Analysis and Discussions

### 6.1. Inference Latency across Different Methods

In Table 2, we compare the inference efficiency of two different representative approaches with our proposed method. Notably, while the CD-based methods result in a significant increase in inference time (2.1 to 3.6 times slower), our ICT incurs virtually no impact on inference efficiency. We attribute this to the fact that both VCD and OPERA either require multiple inference runs or involve substantial additional computations during inference. In contrast, ICT introduces no extra computational cost at inference, further highlighting the advantages of our method.

Method	20-Token Len	50-Token Len	80-Token Len
LLaVA-v1.5	405.3 $\uparrow \times 1.0$	934.6 $\uparrow \times 1.0$	1440.0 $\uparrow \times 1.0$
+ VCD	988.9 $\uparrow \times 2.4$	2031.7 $\uparrow \times 2.2$	3077.5 $\uparrow \times 2.1$
+ OPERA	1371.7 $\uparrow \times 3.4$	3294.1 $\uparrow \times 3.5$	5717.3 $\uparrow \times 3.6$
+ ICT	415.9 $\uparrow \times 1.0$	931.9 $\uparrow \times 1.0$	1485.5 $\uparrow \times 1.0$

Table 2. Comparison of the efficiency of different methods in generating tokens of varying lengths on an NVIDIA H800 GPU. Inference times are recorded in milliseconds.

### 6.2. Generalizability between Different Models

To verify that the derived activation shift vectors to some extent represent the model’s alignment with authenticity, we explored whether these shifts are transferable to other models. Specifically, we applied the activation shift vectors obtained from LLaVA-v1.5 on the COCO random subset to intervene in Qwen-VL. We then evaluated the generalizability of this intervention on the GQA dataset, which has a distribution significantly different from COCO. The results in Table 3 demonstrate that ICT-LLaVA-v1.5 achieves an average improvement of 4.62% in F1 score and 4.64% in accuracy compared to the unmodified model. Additionally, we employed t-SNE to visualize the offset vectors across different layers for LLaVA-v1.5 and Qwen-VL. Figure 4 shows the Object-Level and Image-Level shift vectors of multi-head attention in the 16th and 18th layers for both models. From the figure, we can observe that in layer 16, the Image-Level vectors (blue and yellow) are relatively

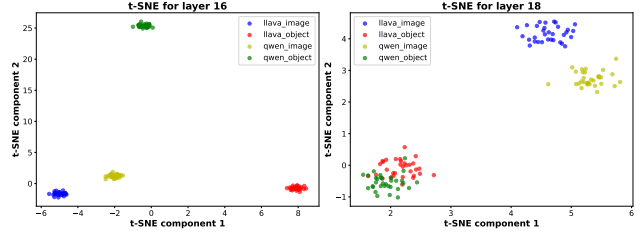


Figure 4. t-SNE visualization of Object-Level and Image-Level offset vectors for LLaVA-v1.5 and Qwen-VL at layers 16 and 18. close to each other, indicating a degree of similarity in encoding Image-Level information between the models. However, the Object-Level vectors (red and green) are more distinct, reflecting model-specific characteristics in encoding fine-grained object details. In layer 18, the Image-Level and Object-Level vectors for both models exhibit high similarity, indicating that the resulting activation shift vectors represent universal shift vectors that guide the model to pay more attention to visual information.

### 6.3. Impact of Hyperparameters on Performance

Our proposed ICT primarily relies on two key hyperparameters: the intervention intensity  $\alpha$  and the number of heads  $K$  involved in the intervention. To investigate the impact of these hyperparameters on performance, we fixed one of the parameters and calculated the average F1 score for LLaVA-v1.5 and Qwen-VL on the POPE COCO random subset. The results are presented in Figure 6, we can observe that when  $\alpha$  is negative—indicating that reverse intervention reduces the model’s attention to visual information—the model’s performance declines. When  $\alpha$  is too small, the model does not receive sufficient intervention, resulting in suboptimal outcomes. Conversely, when  $\alpha$  is excessively large, the intervention becomes too strong, disrupting the model’s foundational capabilities and leading to a decrease in performance. For the hyperparameter  $K$ , we find that when  $K$  is too small, certain attention heads that encode relevant visual information are not ad-

Setting	Method	Accuracy	F1 Score
Random	Regular	80.97	79.01
	VCD	85.59	85.33
	ICT	86.96	86.38
	ICT-LLaVA-v1.5	85.10	83.27
Popular	Regular	75.99	74.84
	VCD	81.83	82.23
	ICT	82.63	82.22
	ICT-LLaVA-v1.5	81.50	80.10
Adversarial	Regular	75.46	74.33
	VCD	80.01	80.75
	ICT	80.83	80.60
	ICT-LLaVA-v1.5	79.73	78.68

Table 3. **Cross-model generalization of ICT.** Performance of Qwen-VL on GQA after applying activation shift from LLaVA-v1.5. ICT-LLaVA-v1.5 refers to the results obtained by applying LLaVA-v1.5’s activation shift vectors to intervene in Qwen-VL.

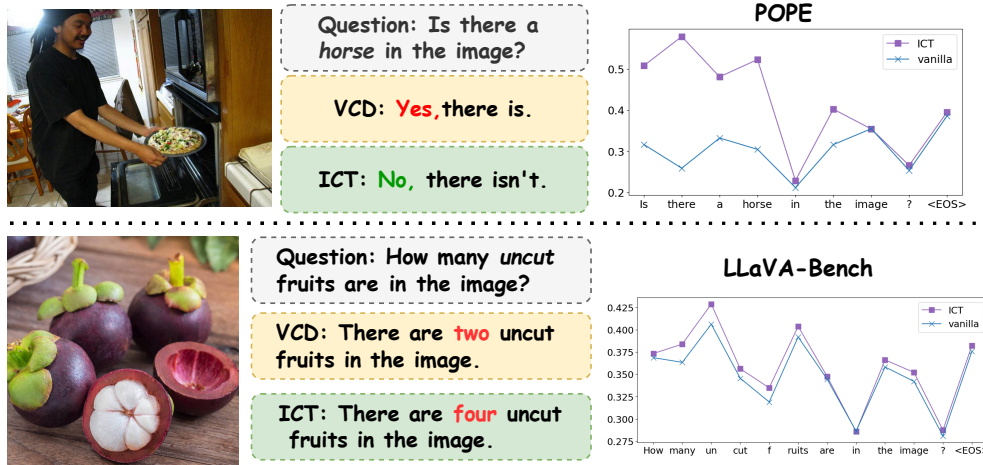


Figure 5. Case Study and Error Analysis of ICT.

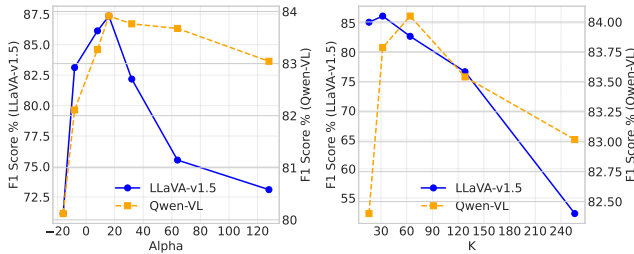


Figure 6. Effect of hyperparameters  $\alpha$  (left) and  $K$  (right) on the F1 score for LLaVA-v1.5 and Qwen-VL models on the POPE COCO random subset.

equately intervened upon, resulting in suboptimal performance. Conversely, when  $K$  is too large, attention heads that encode irrelevant information are unnecessarily interfered with, which leads to performance degradation.

#### 6.4. Analysis of Attention Heads for Visual Information Encoding

In Figure 7, we present the classification accuracy of the binary classifiers for Image-Level and Object-Level features across the 1,024 multi-head attention heads in the 32 layers of LLaVA-v1.5. This analysis helps identify which heads encode overall visual information and which heads capture fine-grained visual details. From the figure, we can observe that the attention heads encoding overall visual information

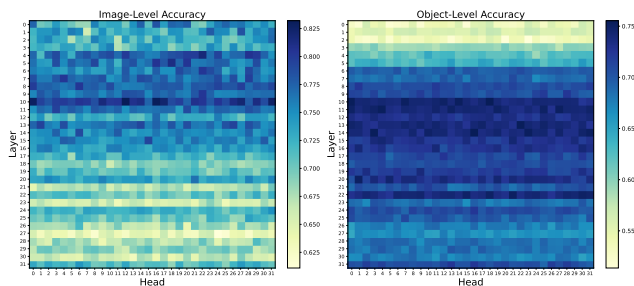


Figure 7. Heatmap of classification accuracy for Image-Level (left) and Object-Level (right) features of LLaVA-v1.5.

are predominantly located in the earlier layers of the model, such as layers 4 and 10. In contrast, the attention heads that capture fine-grained visual details are more concentrated in the later layers, such as layers 20 and 22.

#### 6.5. Case Study and Error Analysis

In Figure 5, we present a case study on the POPE and LLaVA-Bench datasets, visualizing the attention ratio of each question text token to the visual tokens. As illustrated, after applying ICT, the model allocates a higher proportion of attention to visual tokens, especially to object tokens relevant to the question (e.g., “horse” and “fruits”). By prioritizing visual information, ICT correctly identifies the absence of a horse in the image, whereas VCD erroneously concludes that a horse is present due to insufficient attention to visual cues. However, when asked, “How many uncut fruits are in the picture?”, VCD incorrectly answered “two” due to a lack of focus on visual details. Although ICT correctly identifies that there are a total of four fruits in the image, this question requires not only attention to visual content but also reasoning within the text modality. The model needs to not only recognize the overall count of fruits but also focus on the attribute “uncut”. Due to its failure to incorporate this information, ICT outputs a wrong answer.

#### 7. Conclusion and Limitations

In this paper, we mitigate the issue of object hallucinations in LLMs by proposing Image-Object Cross-Level Trusted Intervention (ICT), a training-free, plug-and-play method that enhances the model’s focus on both Image-Level and Object-Level visual information during the forward pass. Our experiments show that ICT significantly reduces hallucinations while also improving general reasoning capabilities. The results confirm that ICT effectively mitigates excessive reliance on language priors, enhancing both accuracy and robustness in diverse visual contexts.

**Limitations.** Our method requires access to the model’s weights, so it cannot be applied to closed-source models. Additionally, we only use Gaussian blur as the transformation method on the image. Future research could explore the use of generative methods for transforming images.

## References

- [1] Renat Aksitov, Chung-Ching Chang, David Reitter, Siamak Shakeri, and Yunhsuan Sung. Characterizing attribution and fluency tradeoffs for retrieval-augmented large language models, 2023. 3
- [2] Jean-Baptiste Alayrac, Jeff Donahue, Pauline Luc, Antoine Miech, Iain Barr, Yana Hasson, Karel Lenc, Arthur Mensch, Katherine Millican, Malcolm Reynolds, et al. Flamingo: A visual language model for few-shot learning. In *Advances in Neural Information Processing Systems*, pages 23716–23736, 2022. 2
- [3] Wenbin An, Feng Tian, Sicong Leng, Jiahao Nie, Haonan Lin, QianYing Wang, Guang Dai, Ping Chen, and Shijian Lu. Agla: Mitigating object hallucinations in large vision-language models with assembly of global and local attention. *arXiv preprint*, 2024. 3
- [4] Wenbin An, Feng Tian, Sicong Leng, Jiahao Nie, Haonan Lin, QianYing Wang, Guang Dai, Ping Chen, and Shijian Lu. Agla: Mitigating object hallucinations in large vision-language models with assembly of global and local attention. *arXiv preprint arXiv:2406.12718*, 2024. 1
- [5] Jinze Bai, Shuai Bai, Shusheng Yang, Shijie Wang, Sinan Tan, Peng Wang, Junyang Lin, Chang Zhou, and Jingren Zhou. Qwen-vl: A versatile vision-language model for understanding, localization, text reading, and beyond. 2023. 1, 2, 5
- [6] Tom Brown, Benjamin Mann, Nick Ryder, Melanie Subbiah, Jared D. Kaplan, Prafulla Dhariwal, Arvind Neelakantan, Pranav Shyam, Girish Sastry, Amanda Askell, et al. Language models are few-shot learners. In *Advances in Neural Information Processing Systems*, pages 1877–1901, 2020. 2
- [7] Beitao Chen, Xinyu Lyu, Lianli Gao, Jingkuan Song, and Heng Tao Shen. Alleviating hallucinations in large vision-language models through hallucination-induced optimization, 2024. 3
- [8] Haozhe Chen, Carl Vondrick, and Chengzhi Mao. Selfie: Self-interpretation of large language model embeddings, 2024. 2
- [9] Zhaorun Chen, Zhuokai Zhao, Hongyin Luo, Huaxiu Yao, Bo Li, and Jiawei Zhou. Halc: Object hallucination reduction via adaptive focal-contrast decoding. In *Forty-first International Conference on Machine Learning*. 1
- [10] Zhaorun Chen, Zhuokai Zhao, Hongyin Luo, Huaxiu Yao, Bo Li, and Jiawei Zhou. Halc: Object hallucination reduction via adaptive focal-contrast decoding, 2024. <http://arxiv.org/abs/2403.00425>. 2, 3
- [11] I.-Chun Chern, Steffi Chern, Shiqi Chen, Weizhe Yuan, Kehua Feng, Chunting Zhou, Junxian He, Graham Neubig, and Pengfei Liu. Factool: Factuality detection in generative ai – a tool augmented framework for multi-task and multi-domain scenarios, 2023. <http://arxiv.org/abs/2307.13528>. 3
- [12] Wei-Lin Chiang, Zhuohan Li, Zi Lin, Ying Sheng, Zhanghao Wu, Hao Zhang, Lianmin Zheng, Siyuan Zhuang, Yonghao Zhuang, Joseph E Gonzalez, et al. Vicuna: An open-source chatbot impressing gpt-4 with 90%\* chatgpt quality. See <https://vicuna.lmsys.org> (accessed 14 April 2023), 2(3):6, 2023. 1, 2
- [13] Jaemin Cho, Seunghyun Yoon, Ajinkya Kale, Franck Dernoncourt, Trung Bui, and Mohit Bansal. Fine-grained image captioning with clip reward. In *Findings of the Association for Computational Linguistics: NAACL 2022*, pages 517–527, 2022. 1
- [14] Yung-Sung Chuang, Yujia Xie, Hongyin Luo, Yoon Kim, James Glass, and Pengcheng He. Dola: Decoding by contrasting layers improves factuality in large language models, 2024. <http://arxiv.org/abs/2309.03883>. 2, 3
- [15] Corinna Cortes. Support-vector networks. *Machine Learning*, 1995. 5
- [16] Li D., Rawat A.S., Zaheer M., Wang X., Lukasik M., Veit A., Yu F., and Kumar S. Large language models with controllable working memory. *arXiv preprint arXiv:2211.05110*, 2022. 3
- [17] Hanxing Ding, Liang Pang, Zihao Wei, Huawei Shen, and Xueqi Cheng. Retrieve only when it needs: Adaptive retrieval augmentation for hallucination mitigation in large language models, 2024. <http://arxiv.org/abs/2402.10612>. 3
- [18] Sebastian Farquhar, Jannik Kossen, Lorenz Kuhn, and Yarin Gal. Detecting hallucinations in large language models using semantic entropy. *Nature*, 630(8017):625–630, 2024. 3
- [19] Javier Ferrando, Gabriele Sarti, Arianna Bisazza, and Marta R. Costa-jussà. A primer on the inner workings of transformer-based language models, 2024. 2
- [20] Chaoyou Fu, Peixian Chen, Yunhang Shen, Yulei Qin, Mengdan Zhang, Xu Lin, Jinrui Yang, Xiawu Zheng, Ke Li, Xing Sun, et al. Mme: A comprehensive evaluation benchmark for multimodal large language models. *arXiv preprint arXiv:2306.13394*, 2023. 5
- [21] Suriya Gunasekar, Yi Zhang, Jyoti Aneja, Caio César Teodoro Mendes, Allie Del Giorno, Sivakanth Gopi, Mojan Javaheripi, Piero Kauffmann, Gustavo de Rosa, Olli Saarikivi, Adil Salim, Shital Shah, Harkirat Singh Behl, Xin Wang, Sébastien Bubeck, Ronen Eldan, Adam Tauman Kalai, Yin Tat Lee, and Yuanzhi Li. Textbooks are all you need, 2023. 3
- [22] Anisha Gunjal, Jihan Yin, and Erhan Bas. Detecting and preventing hallucinations in large vision language models. In *Proceedings of the AAAI Conference on Artificial Intelligence*, pages 18135–18143, 2024. 3
- [23] Anisha Gunjal, Jihan Yin, and Erhan Bas. Detecting and preventing hallucinations in large vision language models. In *Proceedings of the AAAI Conference on Artificial Intelligence*, pages 18135–18143, 2024. 2
- [24] Vipul Gupta, Zhuowan Li, Adam Kortylewski, Chenyu Zhang, Yingwei Li, and Alan Yuille. Swapmix: Diagnosing

- and regularizing the over-reliance on visual context in visual question answering. In *Proceedings of the IEEE/CVF conference on computer vision and pattern recognition*, pages 5078–5088, 2022. 1
- [25] Yudong Han, Liqiang Nie, Jianhua Yin, Jianlong Wu, and Yan Yan. Visual perturbation-aware collaborative learning for overcoming the language prior problem. *arXiv preprint arXiv:2207.11850*, 2022. 1
- [26] Jonathan Ho, Ajay Jain, and Pieter Abbeel. Denoising diffusion probabilistic models. *Advances in neural information processing systems*, 33:6840–6851, 2020. 3
- [27] Wenyi Hong, Weihang Wang, Ming Ding, Wenmeng Yu, Qingsong Lv, Yan Wang, Yean Cheng, Shiyu Huang, Junhui Ji, Zhao Xue, et al. Cogvlm2: Visual language models for image and video understanding. *arXiv preprint arXiv:2408.16500*, 2024. 1
- [28] Haichuan Hu, Yuhan Sun, and Quanjun Zhang. Lrp4rag: Detecting hallucinations in retrieval-augmented generation via layer-wise relevance propagation, 2024. <http://arxiv.org/abs/2408.15533>. 3
- [29] Yingdong Hu, Fanqi Lin, Tong Zhang, Li Yi, and Yang Gao. Look before you leap: Unveiling the power of gpt-4v in robotic vision-language planning. *arXiv preprint arXiv:2311.17842*, 2023. 1
- [30] Lei Huang, Weijiang Yu, Weitao Ma, Weihong Zhong, Zhangyin Feng, Haotian Wang, Qianglong Chen, Weihua Peng, Xiaocheng Feng, Bing Qin, and Ting Liu. A survey on hallucination in large language models: Principles, taxonomy, challenges, and open questions, 2023. 3
- [31] Qidong Huang, Xiaoyi Dong, Pan Zhang, Bin Wang, Conghui He, Jiaqi Wang, Dahua Lin, Weiming Zhang, and Nenghai Yu. Opera: Alleviating hallucination in multimodal large language models via over-trust penalty and retrospection-allocation. In *Proceedings of the IEEE/CVF Conference on Computer Vision and Pattern Recognition*, pages 13418–13427, 2024. 5
- [32] Drew A Hudson and Christopher D Manning. Gqa: A new dataset for real-world visual reasoning and compositional question answering. In *Proceedings of the IEEE/CVF conference on computer vision and pattern recognition*, pages 6700–6709, 2019. 5
- [33] Fushuo Huo, Wenchao Xu, Zhong Zhang, Haozhao Wang, Zhicheng Chen, and Peilin Zhao. Self-introspective decoding: Alleviating hallucinations for large vision-language models, 2024. 3
- [34] Jitesh Jain, Jianwei Yang, and Humphrey Shi. Vcoder: Versatile vision encoders for multimodal large language models. In *Proceedings of the IEEE/CVF Conference on Computer Vision and Pattern Recognition*, pages 27992–28002, 2024. 2
- [35] Juseong Jin and Chang Wook Jeong. Surgical-llava: Toward surgical scenario understanding via large language and vision models. *arXiv preprint arXiv:2410.09750*, 2024. 1
- [36] Junho Kim, Hyunjun Kim, Yeonju Kim, and Yong Man Ro. Code: Contrasting self-generated description to combat hallucination in large multi-modal models, 2024. 2, 3
- [37] Lorenz Kuhn, Yarin Gal, and Sebastian Farquhar. Semantic uncertainty: Linguistic invariances for uncertainty estimation in natural language generation. *arXiv*, 2023. 3
- [38] Junlin Lee, Yequan Wang, Jing Li, and Min Zhang. Multimodal reasoning with multimodal knowledge graph. *arXiv preprint arXiv:2406.02030*, 2024. 2
- [39] Katherine Lee, Daphne Ippolito, Andrew Nystrom, Chiyuan Zhang, Douglas Eck, Chris Callison-Burch, and Nicholas Carlini. Deduplicating training data makes language models better. In *Proceedings of the 60th Annual Meeting of the Association for Computational Linguistics (Volume 1: Long Papers)*, pages 8424–8445, 2022. 3
- [40] Kang-il Lee, Minbeom Kim, Seunghyun Yoon, Minsung Kim, Dongryeol Lee, Hyukhun Koh, and Kyomin Jung. Vlind-bench: Measuring language priors in large vision-language models. *arXiv preprint arXiv:2406.08702*, 2024. 1
- [41] Nayeon Lee, Wei Ping, Peng Xu, Mostofa Patwary, Pascale N Fung, Mohammad Shoeybi, and Bryan Catanzaro. Factuality enhanced language models for open-ended text generation. In *Advances in Neural Information Processing Systems*, pages 34586–34599, 2022. 3
- [42] Seongyun Lee, Sue Hyun Park, Yongrae Jo, and Minjoon Seo. Volcano: Mitigating multimodal hallucination through self-feedback guided revision. *arXiv*, 2024. 3
- [43] Sicong Leng, Hang Zhang, Guanzheng Chen, Xin Li, Shijian Lu, Chunyan Miao, and Lidong Bing. Mitigating object hallucinations in large vision-language models through visual contrastive decoding. In *Proceedings of the IEEE/CVF Conference on Computer Vision and Pattern Recognition*, pages 13872–13882, 2024. 1, 2, 5
- [44] Junnan Li, Dongxu Li, Silvio Savarese, and Steven Hoi. Blip-2: Bootstrapping language-image pre-training with frozen image encoders and large language models. In *Proceedings of the International Conference on Machine Learning*, pages 19730–19742. PMLR, 2023. 2
- [45] Kenneth Li, Oam Patel, Fernanda Viégas, Hanspeter Pfister, and Martin Wattenberg. Inference-time intervention: Eliciting truthful answers from a language model. *Advances in Neural Information Processing Systems*, 36, 2024. 3
- [46] Lei Li, Zihui Xie, Mukai Li, Shunian Chen, Peiyi Wang, Liang Chen, Yazheng Yang, Benyou Wang, Lingpeng Kong, and Qi Liu. Vlfeedback: A large-scale ai feedback dataset for large vision-language models alignment. In *Proceedings of the 2024 Conference on Empirical Methods in Natural Language Processing*, pages 6227–6246, 2024. 2
- [47] Xiang Lisa Li, Ari Holtzman, Daniel Fried, Percy Liang, Jason Eisner, Tatsunori Hashimoto, Luke Zettlemoyer, and Mike Lewis. Contrastive decoding: Open-ended text generation as optimization. *arXiv preprint*, 2023. 3
- [48] Yifan Li, Yifan Du, Kun Zhou, Jinpeng Wang, Xin Zhao, and Ji-Rong Wen. Evaluating object hallucination in large vision-language models. In *The 2023 Conference on Empirical Methods in Natural Language Processing*. 5
- [49] Tsung-Yi Lin, Michael Maire, Serge Belongie, James Hays, Pietro Perona, Deva Ramanan, Piotr Dollár, and C Lawrence Zitnick. Microsoft coco: Common objects in

- context. In *Computer Vision–ECCV 2014: 13th European Conference, Zurich, Switzerland, September 6–12, 2014, Proceedings, Part V 13*, pages 740–755. Springer, 2014. 5
- [50] Bingbin Liu, Jordan T. Ash, Surbhi Goel, Akshay Krishnamurthy, and Cyril Zhang. Exposing attention glitches with flip-flop language modeling, 2023. 3
- [51] Fuxiao Liu, Kevin Lin, Linjie Li, Jianfeng Wang, Yaser Yacoob, and Lijuan Wang. Mitigating hallucination in large multi-modal models via robust instruction tuning. In *The Twelfth International Conference on Learning Representations*, 2023. 3
- [52] Haotian Liu, Chunyuan Li, Yuheng Li, and Yong Jae Lee. Improved baselines with visual instruction tuning, 2023. 1, 2, 5
- [53] Haotian Liu, Chunyuan Li, Qingyang Wu, and Yong Jae Lee. Visual instruction tuning. *Advances in Neural Information Processing Systems*, 36, 2024. 3
- [54] Hanchao Liu, Wenyuan Xue, Yifei Chen, Dapeng Chen, Xiutian Zhao, Ke Wang, Liping Hou, Rongjun Li, and Wei Peng. A survey on hallucination in large vision-language models. *arXiv preprint*, 2024. 2
- [55] Hanchao Liu, Wenyuan Xue, Yifei Chen, Dapeng Chen, Xiutian Zhao, Ke Wang, Liping Hou, Rongjun Li, and Wei Peng. A survey on hallucination in large vision-language models. *arXiv preprint arXiv:2402.00253*, 2024. 1
- [56] Jiajun Liu, Yibing Wang, Hanghang Ma, Xiaoping Wu, Xiaoqi Ma, Xiaoming Wei, Jianbin Jiao, Enhua Wu, and Jie Hu. Kangaroo: A powerful video-language model supporting long-context video input. *arXiv preprint arXiv:2408.15542*, 2024. 1
- [57] Shilong Liu, Zhaoyang Zeng, Tianhe Ren, Feng Li, Hao Zhang, Jie Yang, Chunyuan Li, Jianwei Yang, Hang Su, Jun Zhu, et al. Grounding dino: Marrying dino with grounded pre-training for open-set object detection. *arXiv preprint arXiv:2303.05499*, 2023. 4
- [58] Shi Liu, Kecheng Zheng, and Wei Chen. Paying more attention to image: A training-free method for alleviating hallucination in llms, 2024. 3
- [59] Alexander Nikitin, Jannik Kossen, Yarin Gal, and Pekka Marttinen. Kernel language entropy: Fine-grained uncertainty quantification for llms from semantic similarities. *arXiv*, 2024. 3
- [60] OpenAI. GPT-4. <https://openai.com/gpt-4>, 2023. 2
- [61] Long Ouyang, Jeffrey Wu, Xu Jiang, Diogo Almeida, Carroll Wainwright, Pamela Mishkin, Chong Zhang, et al. Training language models to follow instructions with human feedback. In *Advances in Neural Information Processing Systems*, pages 27730–27744, 2022. 3
- [62] Amandalynne Paullada, Inioluwa Deborah Raji, Emily M. Bender, Emily Denton, and Alex Hanna. Data and its (dis)contents: A survey of dataset development and use in machine learning research. *Patterns*, 2(11):100336, 2021. 3
- [63] Phuc Phan, Hieu Tran, and Long Phan. Distillation contrastive decoding: Improving llms reasoning with contrastive decoding and distillation, 2024. 2, 3
- [64] Venkit P.N., Gautam S., Panchanadikar R., Huang T.H., and Wilson S. Nationality bias in text generation. *arXiv preprint arXiv:2302.02463*, 2023. 3
- [65] Xiaoye Qu, Qiyuan Chen, Wei Wei, Jishuo Sun, and Jianfeng Dong. Alleviating hallucination in large vision-language models with active retrieval augmentation, 2024. <http://arxiv.org/abs/2408.00555>. 3
- [66] Xiaoye Qu, Jiashuo Sun, Wei Wei, and Yu Cheng. Look, compare, decide: Alleviating hallucination in large vision-language models via multi-view multi-path reasoning, 2024. <http://arxiv.org/abs/2408.17150>. 3
- [67] Alec Radford, Jong Wook Kim, Chris Hallacy, Aditya Ramesh, Gabriel Goh, Sandhini Agarwal, Girish Sastry, Amanda Askell, Pamela Mishkin, Jack Clark, et al. Learning transferable visual models from natural language supervision. In *International conference on machine learning*, pages 8748–8763. PMLR, 2021. 1
- [68] Vikas Raunak, Arul Menezes, and Marcin Junczys-Dowmunt. The curious case of hallucinations in neural machine translation. In *Proceedings of the 2021 Conference of the North American Chapter of the Association for Computational Linguistics: Human Language Technologies*, pages 1172–1183, 2021. 3
- [69] Kim S., Cho B., Bae S., Ahn S., and Yun S.Y. Vacode: Visual augmented contrastive decoding. *arXiv preprint arXiv:2408.05337*, 2024. 2, 3
- [70] Lin S., Hilton J., and Evans O. Truthfulqa: Measuring how models mimic human falsehoods. *arXiv preprint arXiv:2109.07958*, 2021. 3
- [71] Yin S., Fu C., Zhao S., Li K., Sun X., Xu T., and Chen E. A survey on multimodal large language models. *arXiv preprint arXiv:2306.13549*, 2023. 3
- [72] Pranab Sahoo, Prabhaskar Meharia, Akash Ghosh, Sriparna Saha, Vinija Jain, and Aman Chadha. A comprehensive survey of hallucination in large language, image, video and audio foundation models. *Findings of the Association for Computational Linguistics: EMNLP 2024*, pages 11709–11724, 2024. 1
- [73] Dustin Schwenk, Apoorv Khandelwal, Christopher Clark, Kenneth Marino, and Roozbeh Mottaghi. A-okvqa: A benchmark for visual question answering using world knowledge. In *European conference on computer vision*, pages 146–162. Springer, 2022. 5
- [74] Lei Shen, Haolan Zhan, Xin Shen, Hongshen Chen, Xiaofang Zhao, and Xiaodan Zhu. Identifying untrustworthy samples: Data filtering for open-domain dialogues with bayesian optimization. In *Proceedings of the 30th ACM International Conference on Information & Knowledge Management*, pages 1598–1608, 2021. 3
- [75] Weijia Shi, Xiaochuang Han, Mike Lewis, Yulia Tsvetkov, Luke Zettlemoyer, and Scott Wen tau Yih. Trusting your evidence: Hallucinate less with context-aware decoding, 2023. 3
- [76] Weijia Shi, Sewon Min, Maria Lomeli, Chunting Zhou, Margaret Li, Rich James, Xi Victoria Lin, Noah A. Smith, Luke Zettlemoyer, Scott Yih, and Mike Lewis. In-context pretraining: Language modeling beyond document boundaries, 2023. 3

- [77] GLM T., Zeng A., Xu B., Wang B., Zhang C., Yin D., Rojas D., Feng G., Zhao H., Lai H., and Yu H. Chatglm: A family of large language models from glm-130b to glm-4 all tools. *arXiv preprint arXiv:2406.12793*, 2024. 2
- [78] Gemma Team, Thomas Mesnard, Cassidy Hardin, Robert Dadashi, Surya Bhupatiraju, Shreya Pathak, Laurent Sifre, Morgane Rivière, Mihir Sanjay Kale, Juliette Love, Pouya Tafti, Léonard Hussenot, Pier Giuseppe Sessa, Aakanksha Chowdhery, Adam Roberts, Aditya Barua, Alex Botev, Alex Castro-Ros, Ambrose Slone, Amélie Héliou, Andrea Tacchetti, Anna Bulanova, Antonia Paterson, Beth Tsai, Bobak Shahriari, Charline Le Lan, Christopher A. Choquette-Choo, Clément Crepy, Daniel Cer, Daphne Ippolito, David Reid, Elena Buchatskaya, Eric Ni, Eric Noland, Geng Yan, George Tucker, George-Christian Muraru, Grigory Rozhdestvenskiy, Henryk Michalewski, Ian Tenney, Ivan Grishchenko, Jacob Austin, James Keeling, Jane Labanowski, Jean-Baptiste Lespiau, Jeff Stanway, Jenny Brennan, Jeremy Chen, Johan Ferret, Justin Chiu, Justin Mao-Jones, Katherine Lee, Kathy Yu, Katie Millican, Lars Lowe Sjoesund, Lisa Lee, Lucas Dixon, Machel Reid, Maciej Mikula, Mateo Wirth, Michael Sharan, Nikolai Chirayev, Nithum Thain, Olivier Bachem, Oscar Chang, Oscar Wahltinez, Paige Bailey, Paul Michel, Petko Yotov, Rahma Chaabouni, Ramona Comanescu, Reena Jana, Rohan Anil, Ross McIlroy, Ruibo Liu, Ryan Mullins, Samuel L Smith, Sebastian Borgeaud, Sertan Girgin, Sholto Douglas, Shree Pandya, Siamak Shakeri, Soham De, Ted Klimenko, Tom Hennigan, Vlad Feinberg, Wojciech Stokowiec, Yu hui Chen, Zafarali Ahmed, Zhitao Gong, Tris Warkentin, Ludovic Peran, Minh Giang, Clément Farabet, Oriol Vinyals, Jeff Dean, Koray Kavukcuoglu, Demis Hassabis, Zoubin Ghahramani, Douglas Eck, Joelle Barral, Fernando Pereira, Eli Collins, Armand Joulin, Noah Fiedel, Evan Senter, Alek Andreev, and Kathleen Kenealy. Gemma: Open models based on gemini research and technology, 2024. 2
- [79] Hugo Touvron, Thibaut Lavril, Gautier Izacard, Xavier Martinet, Marie-Anne Lachaux, Timothée Lacroix, Baptiste Rozière, Naman Goyal, Eric Hambro, Faisal Azhar, et al. Llama: Open and efficient foundation language models. *arXiv preprint*, 2023. 2
- [80] Elena Voita, David Talbot, Fedor Moiseev, Rico Sennrich, and Ivan Titov. Analyzing multi-head self-attention: Specialized heads do the heavy lifting, the rest can be pruned. In *Proceedings of the 57th Annual Meeting of the Association for Computational Linguistics*, pages 5797–5808, 2019. 2
- [81] Zhong W., Feng X., Zhao L., Li Q., Huang L., Gu Y., Ma W., Xu Y., and Qin B. Investigating and mitigating the multimodal hallucination snowballing in large vision-language models. *arXiv preprint arXiv:2407.00569*, 2024. 2, 3
- [82] Guankun Wang, Long Bai, Wan Jun Nah, Jie Wang, Zhaoxi Zhang, Zhen Chen, Jinlin Wu, Mobarakol Islam, Hongbin Liu, and Hongliang Ren. Surgical-llm: Learning to adapt large vision-language model for grounded visual question answering in robotic surgery. *arXiv preprint arXiv:2405.10948*, 2024. 1
- [83] P Wang, S Bai, S Tan, S Wang, Z Fan, J Bai, K Chen, X Liu, J Wang, W Ge, and Y Fan. Qwen2-vl: Enhancing vision-language model’s perception of the world at any resolution. *arXiv preprint arXiv:2409.12191*, 2024. 2
- [84] Xintong Wang, Jingheng Pan, Liang Ding, and Chris Bie-mann. Mitigating hallucinations in large vision-language models with instruction contrastive decoding, 2024. 3
- [85] Sangmin Woo, Jaehyuk Jang, Donguk Kim, Yubin Choi, and Changick Kim. Ritual: Random image transformations as a universal anti-hallucination lever in llms, 2024. <http://arxiv.org/abs/2405.17821>. 3
- [86] Sangmin Woo, Donguk Kim, Jaehyuk Jang, Yubin Choi, and Changick Kim. Don’t miss the forest for the trees: Attentional vision calibration for large vision language models, 2024. 2, 3
- [87] Junfei Wu, Qiang Liu, Ding Wang, Jinghao Zhang, Shu Wu, Liang Wang, and Tieniu Tan. Logical closed loop: Uncovering object hallucinations in large vision-language models, 2024. <http://arxiv.org/abs/2402.11622>. 3
- [88] Kai Wu, Boyuan Jiang, Zhengkai Jiang, Qingdong He, Donghao Luo, Shengzhi Wang, Qingwen Liu, and Chengjie Wang. Noiseboost: Alleviating hallucination with noise perturbation for multimodal large language models, 2024. <http://arxiv.org/abs/2405.20081>. 3
- [89] Xin Xiao, Bohong Wu, Jiacong Wang, Chunyuan Li, Xun Zhou, and Haoyuan Guo. Seeing the image: Prioritizing visual correlation by contrastive alignment, 2024. 3
- [90] Xiaohan Xu, Chongyang Tao, Tao Shen, Can Xu, Hongbo Xu, Guodong Long, and Jian guang Lou. Re-reading improves reasoning in large language models, 2024. <http://arxiv.org/abs/2309.06275>. 3
- [91] L Xue, M Shu, A Awadalla, J Wang, A Yan, S Purushwalkam, H Zhou, V Prabhu, Y Dai, M S Ryoo, and S Kendre. xgen-mm (blip-3): A family of open large multimodal models. *arXiv preprint arXiv:2408.08872*, 2024. 2
- [92] Onoe Y., Zhang M.J., Choi E., and Durrett G. Entity cloze by date: What lms know about unseen entities. *arXiv preprint arXiv:2205.02832*, 2022. 3
- [93] Park Y., Lee D., Choe J., and Chang B. Convis: Contrastive decoding with hallucination visualization for mitigating hallucinations in multimodal large language models. *arXiv preprint arXiv:2408.13906*, 2024. 3
- [94] Zhenjie Yang, Xiaosong Jia, Hongyang Li, and Junchi Yan. Llm4drive: A survey of large language models for autonomous driving. In *NeurIPS 2024 Workshop on Open-World Agents*, 2023. 1
- [95] Shukang Yin, Chaoyou Fu, Sirui Zhao, Tong Xu, Hao Wang, Dianbo Sui, Yunhang Shen, Ke Li, Xing Sun, and Enhong Chen. Woodpecker: Hallucination correction for multimodal large language models. *arXiv preprint*, 2023. 3
- [96] Qifan Yu, Juncheng Li, Longhui Wei, Liang Pang, Wentao Ye, Bosheng Qin, Siliang Tang, Qi Tian, and Yueting Zhuang. Hallucidoctor: Mitigating hallucinatory toxicity in visual instruction data. In *Proceedings of the IEEE/CVF Conference on Computer Vision and Pattern Recognition*, pages 12944–12953, 2024. 3

- [97] Tianyu Yu, Yuan Yao, Haoye Zhang, Taiwen He, Yifeng Han, Ganqu Cui, Jinyi Hu, et al. Rlhf-v: Towards trustworthy mllms via behavior alignment from fine-grained correctional human feedback. In *Proceedings of the IEEE/CVF Conference on Computer Vision and Pattern Recognition*, pages 13807–13816, 2024. 3
- [98] Zihao Yue, Liang Zhang, and Qin Jin. Less is more: Mitigating multimodal hallucination from an eos decision perspective, 2024. <http://arxiv.org/abs/2402.14545>. 3
- [99] Bai Z., Wang P., Xiao T., He T., Han Z., Zhang Z., and Shou MZ. Hallucination of multimodal large language models: A survey. *arXiv preprint arXiv:2404.18930*, 2024. 3
- [100] Han Z., Bai Z., Mei H., Xu Q., Zhang C., and Shou M.Z. Skip: A simple method to reduce hallucination in large vision-language models. *arXiv preprint arXiv:2402.01345*, 2024. 3
- [101] Shaolei Zhang, Tian Yu, and Yang Feng. Truthx: Alleviating hallucinations by editing large language models in truthful space, 2024. 3
- [102] Yi-Fan Zhang, Weichen Yu, Qingsong Wen, Xue Wang, Zhang Zhang, Liang Wang, Rong Jin, and Tieniu Tan. Debiasing multimodal large language models. *arXiv preprint*, 2024. 3
- [103] L Zhao, Y Deng, W Zhang, and Q Gu. Mitigating object hallucination in large vision-language models via classifier-free guidance. 2024. 3
- [104] Zhiyuan Zhao, Bin Wang, Linke Ouyang, Xiaoyi Dong, Jiaqi Wang, and Conghui He. Beyond hallucinations: Enhancing lvlms through hallucination-aware direct preference optimization. *arXiv preprint arXiv:2311.16839*, 2023. 2
- [105] Zheng Zhao, Emilio Monti, Jens Lehmann, and Haytham Assem. Enhancing contextual understanding in large language models through contrastive decoding, 2024. 3
- [106] Lanyun Zhu, Deyi Ji, Tianrun Chen, Peng Xu, Jieping Ye, and Jun Liu. Ibd: Alleviating hallucinations in large vision-language models via image-biased decoding. *arXiv preprint*, 2024. 3
- [107] Wenhao Zhu, Sizhe Liu, Shujian Huang, Shuaijie She, Chris Wendler, and Jiajun Chen. Multilingual contrastive decoding via language-agnostic layers skipping, 2024. <http://arxiv.org/abs/2407.10795>. 2, 3

# ICT: Image-Object Cross-Level Trusted Intervention for Mitigating Object Hallucination in Large Vision-Language Models

## Supplementary Material

### Appendix A: Implementation Details

In our experiments, we used greedy search to ensure reproducibility. Hyperparameter tuning was performed using a grid search to explore the possible combinations of key parameters systematically. The hyperparameters under consideration included  $\alpha$ ,  $\beta$ , and  $K$ . To reduce the dimensionality of the search space, we constrained  $\alpha$  and  $\beta$  to be equal. This constraint is reasonable as these two hyperparameters serve similar roles in our experiments. For LLaVA-v1.5, we applied interventions to the layers `language_model.model.layers.{i}.self_attn.o_proj`, while for Qwen-VL, the interventions were applied to `transformer.h.{i}.attn.c_proj`.

**Grid Search Process** The grid search exhaustively evaluated all combinations of hyperparameters within the specified ranges. Given the aforementioned constraint on  $\alpha$  and  $\beta$ , the search space was defined as the Cartesian product:

$$\{(8, 8), (16, 16), (24, 24), (32, 32)\} \times \{32, 64, 128, 256\}.$$

This resulted in a total of  $4 \times 4 = 16$  unique hyperparameter configurations, which is a relatively small search space.

#### Hyperparameter Search Details

**$\alpha$  and  $\beta$ :** The hyperparameters  $\alpha$  and  $\beta$ , which control the strength of Image-Level and Object-Level intervention, respectively, were allowed to take values from the discrete set  $\{8, 16, 24, 32\}$ . This range was chosen to strike a balance between improving model trustworthiness and maintaining overall performance. By enforcing the constraint  $\alpha = \beta$ , the number of unique combinations was reduced to four, thereby simplifying the search space while ensuring sufficient exploration of the parameter landscape.

**$K$ :** The hyperparameter  $K$ , representing the number of attention heads we intervene on, was explored over the set  $\{32, 64, 128, 256\}$ . This range was determined based on two key considerations:

- Both LLaVA-v1.5 and Qwen-VL architectures consist of 32 layers, each with 32 attention heads, resulting in 1024 total attention heads. The chosen range allows for intervention on varying subsets of these attention heads.
- Preliminary classification accuracy results, as shown in Figure 7, indicate that this range provides sufficient flexibility to cover scenarios from intervening on all heads that are relevant to hallucination to intervening only on those most pertinent to truthfulness.

### Appendix B: More Case Studies

In Figure 8, we present additional illustrative cases from LLaVA-bench to further demonstrate the effectiveness of ICT on extremely challenging open-ended questions. The upper part of Figure 8 vividly illustrates the precision and reliability of our intervention. ICT retains most of the original phrasing, selectively eliminating segments containing untruthful content. This demonstrates that ICT not only significantly reduces the model’s tendency to hallucinate but also achieves this with minimal and minimal side effects.

The lower part of Figure 8 presents another example where ICT successfully preserves and utilizes useful language priors, whereas VCD fails to do so. In this case, both approaches accurately identified the building, but VCD hallucinated incorrect scene opening hours. In contrast, ICT provided suggestions grounded in factual knowledge, leveraging the positive aspects of language priors effectively.



Prompt: Describe this image in detail.

VCD: The painting features a woman with a Mona Lisa-like expression, wearing a black veil. She is the main subject of the painting, and her facial expression is the focal point. The background of the painting is a landscape with a body of water, such as a lake or a river, and a mountain in the distance. There are also two smaller figures in the background, one on the left side and the other on the right side of the painting. The overall composition of the painting is a harmonious blend of the woman's portrait and the natural landscape, creating a captivating visual experience.

ICT: The painting features a woman with a Mona Lisa-like expression, wearing a black veil. She is the main subject of the painting, and her facial expression is the focal point. The background of the painting includes a body of water, such as a lake or a river, and a mountain range. The overall atmosphere of the painting is serene and captivating.



Prompt: What's the best weather, season, time of the day of visiting this place?  
Is the time when this photo was taken a good time to visit this place?

VCD: The best weather, season, and time of the day to visit the Space Needle would be during the spring or summer months, when the weather is pleasant and comfortable. The photo was taken during the day, which is a good time to visit the Space Needle, as it offers better visibility and a more enjoyable experience. However, it is essential to consider the time of day, as the Space Needle is open from 10 am to 10 pm, and visiting during peak hours might be more crowded and less enjoyable.

ICT: The best weather, season, and time of the day to visit the Space Needle would be during the summer months, as the weather is generally warm and pleasant during this time. The photo was taken during the day, which is a good time to visit the Space Needle, as it offers a clear view of the city and the surrounding area. However, it is important to note that the Space Needle is located in Seattle, which can experience cloudy or rainy weather, so it is essential to check the weather forecast before visiting.

Figure 8. More case studies of ICT. In the first example, our ICT avoids captioning non-existent objects in the image while keeping the rest of the caption nearly identical. This demonstrates its ability to refine the accuracy of generated content while maintaining the quality and coherence of the text. In the second example, VCD hallucinated the opening hours of the Space Needle, whereas our ICT correctly retrieved this information from its internal knowledge, stored implicitly within the language modality. This highlights our method's remarkable capability to minimize vision-related hallucinations while leveraging the advantages of language priors.